encit 2020

ABCM Associação Brasileira de Engenharia e Ciências Mecânicas

18th Brazilian Congress of Thermal Sciences and Engineering
November 16-20, 2020 (Online)

ENC-2020-0324
NUMERICAL ANALYSIS OF AN ALTERNATING CURRENT MHD PUMP WITH RECTANGULAR SECTION FOR ELECTROLYTE SOLUTIONS

Matheus A. M. Campos
Department of Mechanical Engineering, POLI/COPPE, Federal University of Rio de Janeiro, Cid. Universitária, Rio de Janeiro, Brazil
matheusamc@poli.ufrj.br

Gabriel L. Verissimo
Department of Mechanical Engineering, POLI/COPPE, Federal University of Rio de Janeiro, Cid. Universitária, Rio de Janeiro, Brazil
gabrielverissimo@mecanica.coppe.ufrj.br

Marcelo J. Colaço
Department of Mechanical Engineering, POLI/COPPE, Federal University of Rio de Janeiro, Cid. Universitária, Rio de Janeiro, Brazil
colaco@asme.org

Abstract. Magnetohydrodynamics (MHD) pumps are the ones that use the Lorentz force, which arises when a conducting fluid is subjected to a magnetic field and an electric current, as a driving force. These pumps are restricted to electrical conducting fluids such as molten salts, liquid metals and electrolyte solutions. When pumping electrolyte solutions under the action of direct currents (DC), electrolysis can be induced causing bubbles formation and accelerated electrodes consumption. These effects, however, can be reduced or eliminated by using alternating currents (AC). In this work, an AC MHD pump for electrolyte solutions is evaluated aiming to study the velocity and pressure fields for different current frequencies. Temperature behaviour is also evaluated during transient simulations. Electromagnetic and fluid dynamic equations are solved, considering the Lorentz force and the Joule heating effect. The ANSYS FLUENT software was used to solve the problem. The electric potential, magnetic field, Lorentz force, and Joule heating effect equations were added in the FLUENT software through User-Defined Functions (UDF) and User-Defined Scalar (UDS). Laminar and turbulence models were compared during verification and the best model was selected to perform the simulation.

Keywords: *MHD, MHD Pump, Numerical Simulation, Computational Fluid Mechanics*

1. INTRODUCTION

The Magnetohydrodynamics (MHD) is the study of electrical conducting fluid flows in the presence of magnetic and/or electric fields (Davidson, 2001). An interesting application of the MHD theory in engineering is the MHD pump, which uses the Lorentz force that arises from the interaction between the fluid, the imposed magnetic field and the electric current. The imposed electric current can be either direct or alternating, leading these pumps to be divided into two classes: DC (direct current) or AC (alternating current) MHD pumps.

MHD pumps show some advantages compared to their mechanical counterparts, such as simple and compact construction, absence of moving parts, and capacity of handling high temperatures. These features in turn promote a reduction in the required maintenance, higher reliability and noise reduction (Al-Habahbeh, 2016; Martynovich, 2018). Some of these advantages make possible to use these pumps as alternatives to the conventional ones when pumping some dangerous fluids, molten metals and molten salts. In contrast, according to Al-Habahbeh (2016), MHD pumps presents some disadvantages as reverse flow at the end of the magnetic field, high construction costs due magnets price, lack of accurate analytical models, non-homogeneous velocity profiles distribution and instabilities of the flow-field in certain operating conditions.

This work is focused on applications where seawater is the working fluid. When pumping this kind of solution, an additional difficult arises since electrolysis is induced when using direct current. Consequently, there are bubbles formation and accelerated electrodes consumption, which compromises the pump operation (Hughes *et al*., 1995; Jang and Lee, 1999; Boissonneau and Tibault, 1999; Lemoff and Lee, 2000; Ho, 2007). Some attempts to extinguish or reduce the electrolysis effect over the fluid flow have been made, e.g. the bubble isolation systems created by Homsy *et al*. (2005) and Nguyen and Kassegne (2007), and the use of alternating currents that can inhibit electrolysis reactions as proposed by Lemoff and Lee (2000) and Lee and Lemoff (2003).

However, the use of alternating current implies in a different configuration for the pump compared with the cases where direct current is used. In DC MHD pumps both electric current and magnetic fields are steady in order to guarantee a flow in a fixed direction. To reach the same unidirectional flow in AC MHD pumps, it is necessary to apply a time varying magnetic

field in the same frequency as the applied electric current. In this work, the operation of an AC MHD pump with low frequencies for electrolyte solutions is evaluated, aiming to study the implications of alternating current and time varying magnetic fields on the velocity and pressure field. Joule heating is considered during simulations and its effect over the fluid temperature is also evaluated. The studied geometry is inspired by the one proposed by Aoki *et al*. (2013), shown on Fig. 1. The straight section where the MHD pump is located can be seen in Fig. 2, where the electrodes positions are highlighted in red.

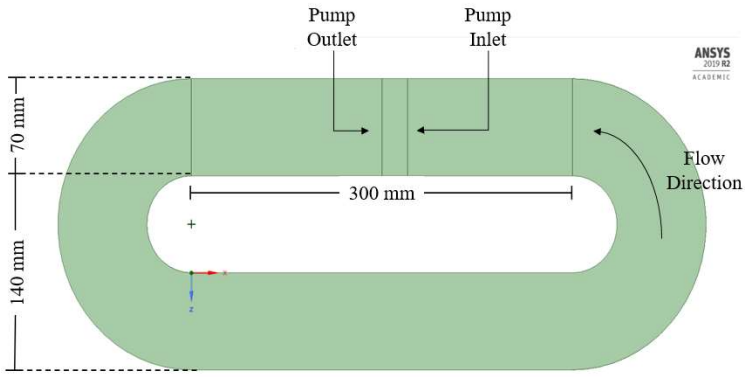

Figure 1. Superior view from the studied channel.

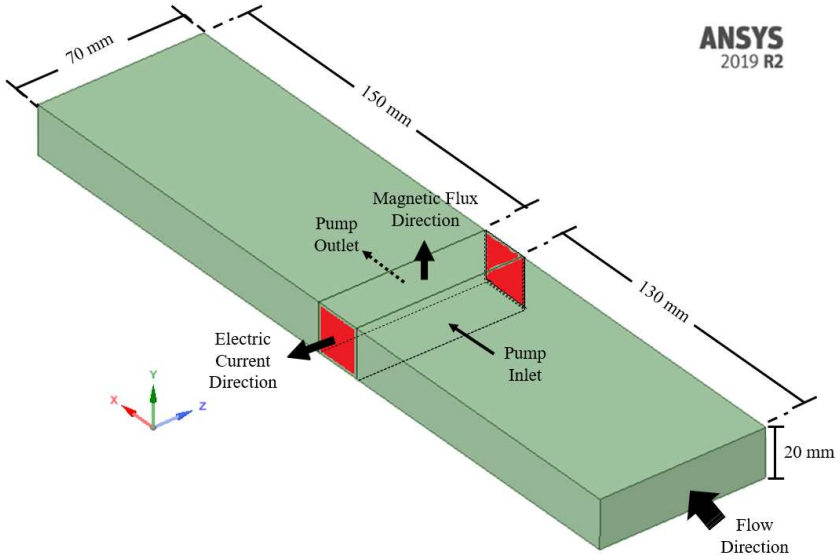

Figure 2. Highlighted channel straight section.

2. MATHEMATICAL MODEL

2.1 Governing equations

The proposed mathematical model is based on the one presented by Davidson (2001). The electromagnetic equations in MHD are composed by the Ohm's law, charge conservation equation, Faraday's law, Gauss' law for magnetic fields, and pre-Maxwell Ampère's law, given by Eqs. (1) – (5).

$$\mathbf{J} = \sigma(\mathbf{E} + \mathbf{u} \times \mathbf{B}) \tag{1}$$

$$\nabla \cdot \mathbf{J} = 0 \tag{2}$$

$$\nabla \times \mathbf{E} = -\frac{\partial \mathbf{B}}{\partial t} \tag{3}$$

$$\nabla \cdot \mathbf{B} = 0 \tag{4}$$

$$\nabla \times \mathbf{B} = \mu_m \mathbf{J} \tag{5}$$

where **J** is the current density, **E** is the electric field, **B** is the magnetic flux density, **u** is the velocity vector, σ is the electrical conductivity and μ_m is the magnetic permeability.

Due to the different nature of the electric field, it is of interest to split it in two terms: the electrostatic part of the field, that can be written as a function of an electrostatic potential, V, and the electric field induced by the time varying magnetic field, $\mathbf{E}_i$. The Ohm's law can be rewritten as presented in Eq. (6). From this equation, and considering Eq. (2), it is possible to derive the electric potential Poisson equation, Eq. (7).

$$\mathbf{J} = \sigma(-\nabla V + \mathbf{E}_i + \mathbf{u} \times \mathbf{B}) \tag{6}$$

$$\nabla^2 V = \nabla \cdot (\mathbf{u} \times \mathbf{B}) \tag{7}$$

Due to low frequencies, low magnetic flux densities, low velocities considered in this work, and the physical properties of the studied fluid, the electric fields induced as a consequence of the time varying magnetic field and fluid motion in the presence of a magnetic field are very low. Thus, during this work it is considered that the induced electric fields are neglected before the one imposed by the electric potential. Due to this simplifications, the electrical current density depends only on the electrical potential determination, Eq.(7), to be calculated by Eq. (6). From Eqs. (1), (3) and (5), it is possible to derive a transport equation for the magnetic field known as a magnetic induction equation. Despite this result, due to computational limitations it is assumed that the magnetic flux density is constant all over the interested domain and therefore this result is not of interest for the present work. Therefore, to achieve the present work objectives, Ohm's law, Eq. (6), and the Poisson equation for electrical potential, Eq. (7), form the set of electromagnetics equations needed to the MHD Pump modelling.

In this work it is assumed that the fluid is Newtonian and the flow is incompressible, then the continuity, momentum and energy conservation equations, assuming the Lorentz force and Joule heating effect, are written, respectively, as,

$$\nabla \cdot \mathbf{u} = 0 \tag{8}$$

$$\frac{D\mathbf{u}}{Dt} = -\nabla p + \mu \nabla^2 \mathbf{u} + \mathbf{J} \times \mathbf{B} + \rho \mathbf{g} \tag{9}$$

$$\rho \frac{De}{Dt} = \rho \phi + \kappa \nabla^2 \mathrm{T} + \frac{\mathbf{J} \cdot \mathbf{J}}{\sigma} \tag{10}$$

where ρ is the fluid density, μ is the fluid dynamic viscosity, κ is the fluid thermal conductivity, p is the pressure, **g** is the gravitational acceleration vector, ϕ is the mechanical dissipation, e is the internal energy, and T is the temperature.

In the momentum equation, Eq. (9), the Lorentz force is accounted as a body force. Furthermore, in the energy conservation equation, Eq. (10), it is inserted a heat source term for the Joule heating effect. The coupling between fluid mechanics equations, Ohms law and electrical Poisson equation completes the set of equations.

2.2 Boundary conditions

It important to let it clear that in this work, two situations occur. During model's validation the complete geometry presented in Fig. 1 is evaluated, while during alternating current analysis it is considered only a portion of the straight channel section. It leads to a different set of boundary conditions. In both cases, in order to solve the electrical Poisson equation, Eq. (7), imposed electric potentials are specified in the electrode's positions, and any region different from this is considered to be electrical insulate. For the validation case, in which a DC MHD pump is evaluated, a fixed value is set in one electrode while the other is set null. For the AC MHD pump simulations, a peak value, V_0, is selected and it varies over time in a sinusoidal form, Eq. (11), in one electrode at a frequency f, while the other is set null. It is important to highlight that the magnetic density flux varies synchronously with the applied electric potential.

$$V = V_0 . \sin(2\pi f t) \tag{11}$$

For the solid walls (channel side and bottom walls), impenetrable and non-slip boundary conditions are specified for the mass and momentum conservation equations. The channel top boundary is considered to be open, and a stress-free boundary condition is specified. These conditions are the same for the two cases considered.

When simulating the short section of the channel, for the alternating current analysis, Fig.3, two additional conditions must be specified for the channel inlet and outlet. In the channel inlet, total pressure is specified, while in the channel outlet, static pressure is specified. In both conditions the value set is 101.325 kPa.

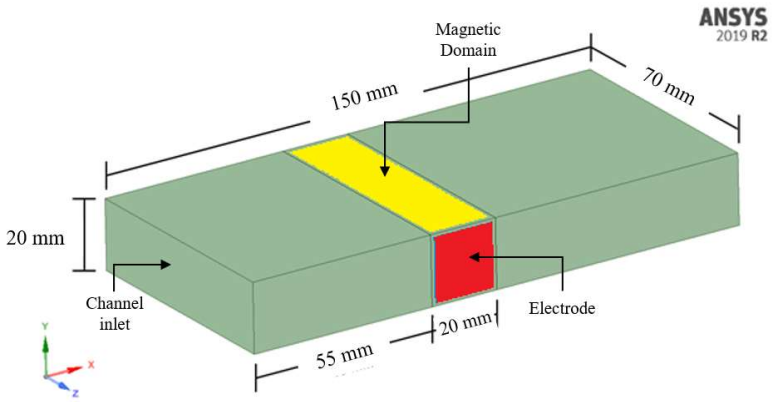

Figure 3. Studied channel during alternating current analysis.

For the energy equation it is considered a critical case where every wall in the channel is thermally insulated during alternating current simulations, and the fluid enters the channel at 300 K. During validation, the thermal boundary conditions were specified in an attempt to match the ones set by Aoki (2011) during his experiments, although they are not clear. Therefore, it is specified a convective heat transfer boundary condition in every wall of the circuit, Fig. 1, with a global heat transfer coefficient of 20 W/m^2 and ambient temperature of 300 K. Seawater properties are presented in Tab. 1.

Table 1. Seawater properties.

Electrical conductivity	Density	Thermal conductivity	Dynamic viscosity
5 S/m	1020 kg/m^3	0.6 W/m.K	1.09 x 10^{-3} Pa.s

3. NUMERICAL SIMULATIONS

3.1 Numerical implematation

In the present work, geometry design, mesh and physical modelling were made in ANSYS 2019 R2. The ANSYS FLUENT 2019 R2 software adopts the finite volume approach and it was used to solve mass, momentum, energy conservation and electric potential equations. Electric Poisson equation was inserted as a scalar transport equation using UDSs (User Defined Scalars), a tool that allows the insertion of additional transports equations. The momentum equation was modified through UDFs (User Defined Functions) that allows the insertion of additional source terms in the equation, as the Lorentz force. The same method was used to introduce the Joule effect heating source term in the energy conservation equation. Both UDSs and UDFs were written in C language. The magnetic flux density was considered uniform and known in the entire domain over time. This numerical implementation is based on the work from Verissimo *et al*. (2018).

Table 2. Meshing parameters.

Model	Element. Size [m]	Number of Layers	Growth Rate	Max. Thickness [m]
Laminar	0.0025	10	1.10	0.001
Standard k-ε	0.003	16	1.05	0.005
Realizable k-ε	0.003	16	1.05	0.005
RNG k-ε	0.005	10	1.05	0.005
Standard k-ω	0.005	16	1.05	0.005
SST k-ω	0.005	10	1.05	0.005
Transition SST	0.002	16	1.05	0.005

The implemented models' results are verified in comparison to the ones presented by AOKI *et al*. (2013) for a DC MHD pump with an applied voltage of 20 V on the electrodes. During this step, six different RANS (Reynolds Average Navier-Stokes) turbulent models are evaluated: Standard k-ε (Pope, 200), Realizable k-ε (Shih *et al*., 1994), RNG k-ε (Roman, 2014), Standard k-ω (Wilcox, 1994), SST k-ω (Menter, 1994) and Transition SST (Langtry, 2006). During mesh generation, the

Inflation tool available in ANSYS *meshing* was used to improve mesh quality close to the channel walls (ANSYS Inc., 2013). For each model, a different mesh refinement was selected due to convergence analysis and the selected parameters for each mesh generation are presented in Tab. 2. This set of parameters resulted in meshes with 720,773, 648,350, 648,350,153,157, 224,651, 153,157 and 1,472,035 elements, respectively.

3.2 Validation

The validation consisted in a comparison between simulated results in accordance with the presented guidelines and experimental data available in the work of Aoki (2011). The comparison is shown on Fig. 4, for a DC MHD pump operating at 12 V, 20V and 30 V. In his work, Aoki (2011) specifies the magnets pair as a NdFeB N35 with a magnetic flux density of 0.3 T. Therefore, during simulations, the known magnetic flux density was set at 0.3 T in the MHD pump region.

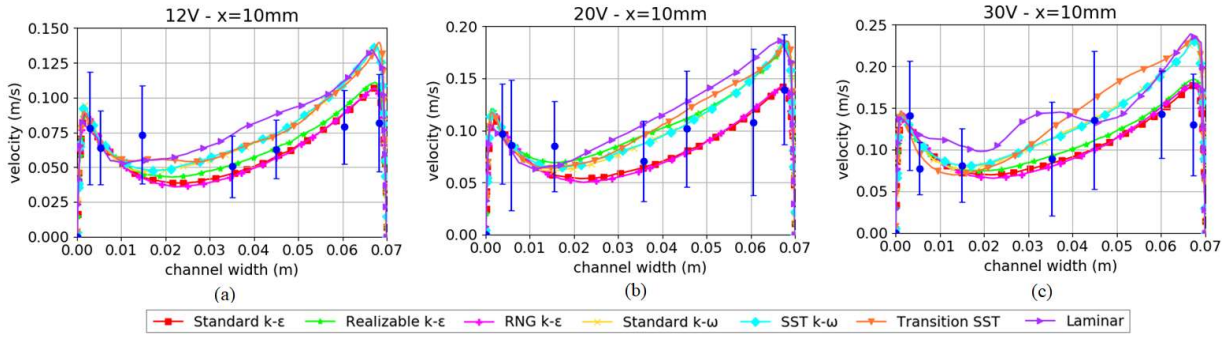

Figure 4. Comparison between simulation results and experimental data (AOKI,2011): (a) 12 V; (b) 20 V.

Figure 4 shows experimental data collected by Aoki (2011) and the simulated results measured 10 mm after the pump outlet and at half height. The "M" velocity profile can be seen in simulated results, in agreement with Aoki (2011) observations. A reasonable agreement between experimental data and simulated results is found. There are some differences between numerical results obtained for each turbulence models. Therefore, the model chosen was the one with the best agreement between simulated and experimental data, also considering the computational cost. From this point on, simulations proceed with RNG k-ε model, once this model presents a good agreement with experimental data and requires meshes with less refinement.

A qualitative validation was made for the energy equation, also based on experimental data presented by Aoki (2011). The comparison between simulated results and experimental data is presented in Tab. 3, and shows a satisfactory agreement between them.

Table 3. Energy equation qualitative validation.

Applied voltage	Experimental temperature [K]	Simulated temperature [K]	Relative difference [%]
12 V	301.45	302.73	0.43
20 V	306.25	307.49	0.40
30 V	319.85	316.72	0.98

4. RESULTS AND DISCUSSION

In order to evaluate the influence of alternating currents in AC MHD pumps, velocity, pressure and temperature profiles are obtained for a peak-applied voltage of 30 V with frequencies of 1 Hz, 10 Hz and 50 Hz. It is also of interest to evaluate Lorentz force and current density behaviors during these transient simulations. At this frequency range, induced currents can be neglected, and it is only considered the electrostatic current. The evaluated channel is the one presented in Fig. 3, and the boundary conditions are the ones detailed in section 2.3. The magnetic flux density is assumed to be known over the entire domain, null outside MHD pump region and constant inside the pump domain. The peak magnetic flux density is set as 0.3 T and varies synchronously with the applied voltage. Current density, Lorentz force, velocity and temperatures are evaluated along the channel's width at pump's outlet, and pressure is evaluated along channels length in its center. In order to properly evaluate the alternating current influence over the flow, results are compared to an equivalent DC case where the same time averaged Lorentz force. It occurs when an electrical potential difference of 15 V is applied in the DC MHD pump electrodes and a steady magnetic density flux of 0.3 T is considered.

Figure 5 shows the current density value measured at pump's outlet distributed over channels width for each evaluated frequency. The presented results are measured during a complete period of voltage oscillation, in order to properly compare the different frequencies.

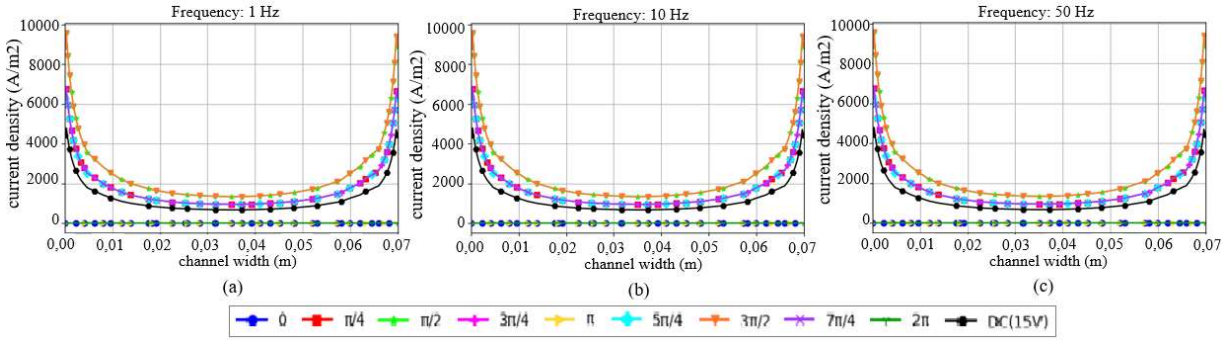

Figure 5. Current density in investigated cases.

One can notice that no significant difference between the evaluated current densities is found for the applied frequencies. Noticing that Lorentz force depends on current density to be obtained, once there is no significant difference in this quantity for the evaluated frequencies, and considering that a constant synchronous magnetic flux density is assumed, it is expected that the same behavior occur with the current densities. This can be observed in Fig 6, where the Lorentz force results are presented.

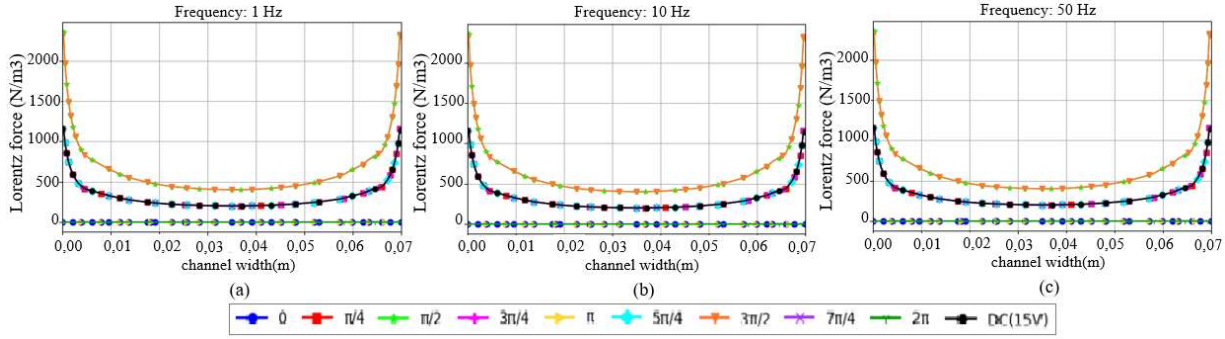

Figure 6. Lorentz force in investigated cases.

The same profile is obtained for current density and Lorentz force, and these profiles matches for both DC and AC cases. As can be seen in Fig. 5 and Fig. 6, higher values are found close to the walls, where higher electric potential differences occur, which leads to higher density current values, and, consequently, higher Lorentz force values. In contrast, close to the channel's center, electric potential difference tends to be more uniform, then lower current densities and Lorentz forces values appear. It is important to notice that due to the oscillating applied voltage and magnetic flux density, these two quantities also oscillate over time.

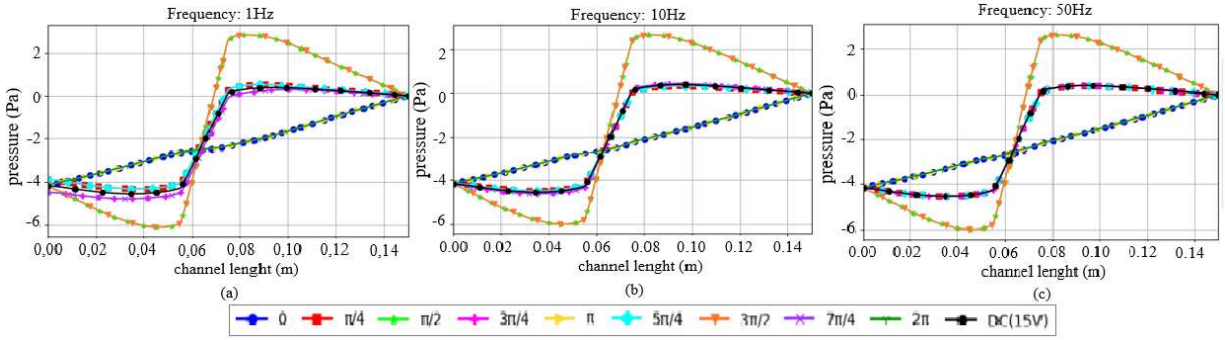

Figure 7. Pressure in investigated cases.

Figure 7 shows results for pressure distribution along channels length. It can be observed that the profile for AC cases matches the one formed in DC configuration, although it oscillates over time. While for current density and Lorentz force the observed oscillation is symmetric over the evaluated period, this does not happen for pressure due to inertia effects. One can also notice that while for these two first quantities there is no observed difference in the results for the three evaluated frequencies, for pressure results a significant difference is encountered.

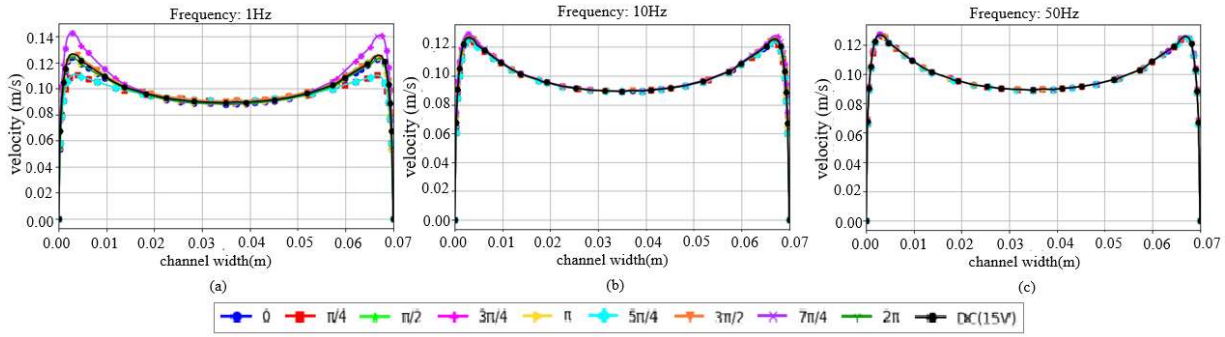

Figure 8. Velocity in investigated cases.

Figure 8 shows the velocity profile formed at pump´s outlet. The "M" velocity profile is formed due to Lorentz force action over the fluid. For the highest frequencies evaluated, there is a satisfactory agreement between direct current and alternating current cases when the voltage equivalency is respected. Mainly, it is possible to observe that for frequencies over 10 Hz there is a lower amplitude oscillation of velocity, while for a frequency of 1 Hz a significantly oscillation amplitude is found. In every case, the time averaged velocity profile matches with the direct current equivalent results.

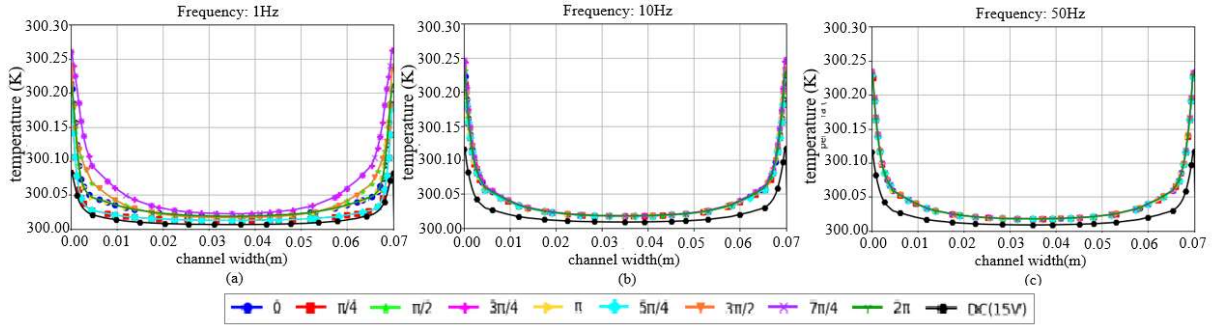

Figure 9. Temperature in investigated cases.

Temperature results at pump's outlet, Fig. 9, show the same profile observed in Fig. 5 for current density. Highest temperatures are achieved close to the walls where electrodes are located, and current density is more intense. The observed profiles match for both alternating and direct current cases, although higher temperatures are reached in ACconfiguration. One can notice that in this simulated case where the fluid is constantly renewed inside the channel, there is no relevant heating, while for the validation cases where a closed circuit is simulated it is. Therefore, depending on the MHD pump application, temperature may be a sensible variable, particularly in AC configurations.

As a complement to the conduct analysis, it is possible to obtain the MHD pump efficiencies as shown by Verissimo et al. (2018). Considering proposed equivalence between an AC and DC configuration, it is possible to show that the required electrical power when applying alternating current is twice the one required in a direct current configuration. Consequently, the achieved efficiencies are 0.01 % and 0.005%, respectively for the DC and AC configurations. These efficiencies have the same order as the ones found by Verissimo et al. (2018), in whose work the maximum efficiency found for an helicoidal MHD DC pump are around 0.0085 %.

5. CONCLUSIONS

This work presented a numerical simulation of a rectangular section AC MHD pump operating with an electrolyte solution, with the aim to investigate the influence of the alternating current on the fluid flow. Frequencies 1 Hz, 10 Hz and 50 Hz were tested for an applied peak voltage of 30 V, with a uniform magnetic field of 0.3 T. The current density,

Lorentz force, pressure, velocity, and temperature distribution at specific locations inside the channel were presented in order to compare this AC configuration with an equivalent DC configuration where a 15 V voltage is applied.

It was show that for current density, Lorentz force, pressure, and temperature there is an oscillatory behavior for every evaluated frequency in AC cases. Furthermore, there is a satisfactory agreement between the AC cases results and the equivalent DC case. The augmentation of the frequency seems to reduce the oscillations amplitude of the velocity profile and, for frequencies from 10 Hz to above, no significant variation is found, leading to a satisfactory agreement with the DC case. Additionally, it is show that an AC configurations results in higher temperatures due Joule effect heating and lower pumping efficiency.

6. REFERENCES

Al-Habahbeh, O.M., Al-Saqqa, M., Safi, M. and Khater, T.A., 2016. *Review of magnetohydrodynamic pump applications*.

ANSYS Inc., 2013. "ANSYS Fluent Theory Guide".

Aoki, L.P., 2001. *Estudo do Efeito Magnetohidrodinâmico em um Eletrólito a Partir do Uso de um Disposistivo Ejetor Eletromagnético*. São Carlos: Universidade de Sâo Paulo.

Aoki, L.P., Schulz, H.E. and Maunsell, M. G., 2013. *An MHD Study of Behavior of an Electrolyte Solution using 3D Numerical Simulation and Experimental Results*. Boston, COMSOL.

Boissonneau, P. and Thibault, J.P., 1999. *Experimental analysis of coupling between electrolysis and hydrodynamics in the context of MHD in seawater*. J. Phys. D: Appl. Phys., Volume 32, pp. 2387-2398.

Davidson, P.A., 2001. *An Introduction to Magnetohydrodynamics*. s.l.:Cambridge University Press.

Ho, J.H., 2007. *Characteristic Study of MHD Pump with Channel in Rectangular Ducts. Journal of Marine Science and Technology*, 15(4), pp. 315-321.

Homsy, A, Koster S., Eijkel, J.C.T., Berg, A., Lucklum, F., Verpoorte, E. and Rooij, N. F.., 2005. *A High Current Density DC Magnetohydrodynamic (MHD) Micropump*. Lab Chip, Volume 5, pp. 466-471.

Hughes, M., Pericleous, K.A. and Cross, M., 1995. *The numerical modelling of DC electromagnetic pump and brake flow*. Applied Mathematical Modelling, 19(12), pp. 713-723.

Jang, J. and Lee, S.S., 2000. *Theoretical and experimental study of MHD (magnetohydrodynamic) micropump*. Sensor and Actuators, Volume 80, pp. 84-89.

Langtry, R. B., 2006. *A Correlation-Based Transition Model using Local Variables for Unstructured Parallelized CFD codes*. Institut für Thermische Strömungsmaschinen und Maschinenlaboratorium Universität Stuttgart , 31 May.

Lemoff, A.V. and Lee, A.P., 2000. "AC magnetohydrodynamic micropump," Sens. Actuators B, 63(3), pp. 178-185.

Lemoff, A.V. and Lee, A.P., 2003. *An AC Magnetohydrodynamic Microfluidic Switch for Micro Total Analysis Systems*. Biomedical Microdevices, Volume 5, pp. 55-60.

Martynovich, I., Avdeev, A. and Drobotov, A., 2018. *Magnetohydrodynamic Pump Work Simulation*. s.l., s.n.

Menter, F. R., 1994. *Two-Equation Eddy-Viscosity Turbulence Models for Engineering Applications*. AIAA Journal, 32(8), pp. 1598-1605.

Nguyen, B. and Kassegne, S., 2008. *High-current density DC magenetohydrodynamics micropump with bubble isolation and release system*. Microfluid Nanofluid, Volume 5, pp. 383-393.

Pope, S.B., 2000. *Turbulent Flows*. 1 ed. s.l.:Cambridge University Press.

Roman, C.R., 2014. *Study of the electromagnetic pumping systems of molten metals and molten salts*. Grenoble: Université de Grenoble.

Shih, T. H., Liou, W.W., Shabbir, A, Yang, Z and Zhu J. ., 1995. *A new k-ϵ eddy viscosity model for high reynolds number turbulent flows*. Computers & Fluids, 24(3), pp. 227-238.

Verissimo, G.L., Pacheco, C.C., Colaco, M.J., Leiorz, A.J.K., Cruz, M.E.C., Santos, H.F.L. and Defilippo, M., 2018. *Three-Dimensional Numerical Simulations of Helicoidal MHD Pumps*. Beijing, Proceedings of the 16th International Heat Transfer Conference.

Wilcox, D.C., 1994. *Turbulence Modelling for CFD*. California: DCW Industries.

7. RESPONSIBILITY NOTICE

The authors are the only responsible for the printed material included in this paper.